

# A CONTINUOUS MULTIPLE HYPOTHESIS TESTING FRAMEWORK FOR OPTIMAL EXOPLANET DETECTION

BY NATHAN C. HARA<sup>1</sup>, THIBAUT DE POYFERRÉ<sup>2</sup> JEAN-BAPTISTE DELISLE<sup>1</sup> MARC HOFFMANN<sup>3</sup>

<sup>1</sup>*Observatoire Astronomique de l'Université de Genève, 51 Chemin de Pegasi b, 1290 Versoix, Switzerland, nathan.hara@unige.ch*

<sup>2</sup>*Mathematical Science Research Institute, Berkeley, USA*

<sup>3</sup>*University Paris-Dauphine, CEREMADE, Place du Maréchal De Lattre de Tassigny, 75016 Paris, France*

The detection of exoplanets is hindered by the presence of complex astrophysical and instrumental noises. Given the difficulty of the task, it is important to ensure that the data are exploited to their fullest potential. In the present work, we search for an optimal exoplanet detection criterion. We adopt a general Bayesian multiple hypothesis testing framework, where the hypotheses are indexed by continuous variables. This framework is adaptable to the different observational methods used to detect exoplanets as well as other data analysis problems. We describe the data as a combination of several parametrized patterns and nuisance signals. We wish to determine which patterns are present, and for a detection to be valid, the parameters of the claimed pattern have to correspond to a true one with a certain accuracy. We search for a detection criterion minimizing false and missed detections, either as a function of their relative cost, or when the expected number of false detections is bounded. We find that if the patterns can be separated in a technical sense, the two approaches lead to the same optimal procedure. We apply it to the retrieval of periodic signals in unevenly sampled time series, emulating the search for exoplanets in radial velocity data. We show on a simulation that, for a given tolerance to false detections, the new criterion leads to 15 to 30% more true detections than other criteria, including the Bayes factor.

**1. Introduction.** The study of planets outside of the solar system, or exoplanets, emerged as a scientific field with the discovery of planets orbiting a pulsar (Wolszczan and Frail, 1992), and its development was further accelerated with the detection of 51 Peg b, a planet orbiting a Sun-like star (Mayor and Queloz, 1995). The latter was discovered with an observational method consisting in measuring the velocity of a given star projected onto the line of sight, or radial velocity, thanks to the Doppler effect. Since then, several observational techniques were developed, each sensitive to planets of different masses and orbital periods, and capable of measuring different physical parameters. There are other observational methods, in particular transits, imaging, astrometry, and gravitational microlensing (e.g. Perryman, 2018).

In all these techniques, the data might show the signatures of one or several planets, buried in complex noises. All the planetary signals are parametrized in the same way. Depending on the techniques, this might be by the orbital period, eccentricity, phase, or the centroid position in an image, also the planet parameters: radius, mass etc. In all cases, the goal is to determine how many planets can be confidently detected and what their characteristics are with a certain accuracy: if the orbital elements of a claimed planet are too far from a planet truly in the system, it might lead to incorrect scientific conclusions. For instance, with radial velocities, the presence of an orbiting planet causes a reflex motion of the star, which, as a

---

*Keywords and phrases:* Exoplanets, Bayesian, False discovery rate, Decision theory, Maximum utility.

result moves back and forth towards the observer, and thus periodic radial velocity variations should be observed. If several planets are present, in first approximation the data can be described by the sum of their individual contributions. If a planet is detected with the wrong orbital period, it can be considered as a false detection even if the correct number of planets is claimed. Due to the similarities between these different problems, we adopt a theoretical model which encompasses the different exoplanet observational techniques.

We reason in a general framework, and replace the particular case of exoplanets with a general parametric model. The central assumption of our work is that the data  $y$  is described by  $n = 0$  to  $n_{max}$  signals with the same parametric model, which we call patterns, and nuisance signals parametrized by  $\eta$ . These nuisance signals might include deterministic ones: offsets, trends... as well as stochastic ones. In the latter case  $\eta$  would include the noise amplitude, time-scales, spatial correlation etc. The pattern  $i$  is described by the parameters by  $\theta_i$ . The variables  $n, (\theta_i)_{i=1..n}, \eta$  are unknown and the likelihood is then of the form  $p(y | (\theta_i)_{i=1..n}, \eta)$ . We further assume that we have prior distributions for our variables.

We not only want to determine the number of patterns  $n$ , but also what they are. This problem can be interpreted as testing multiple hypotheses, but instead of considering  $m$  discrete hypotheses  $H_i, i = 1..m$ , our hypotheses are of the form: “there are  $n$  pattern whose parameters are in the regions  $(\Theta_i)_{i=1..n}$ ”. The hypotheses are indexed by the choice of the parameter space regions  $(\Theta_i)_{i=1..n}$ , where each  $\Theta_i$  is typically a ball of fixed radius and centered on  $\theta_i$ . In the case of exoplanets,  $\theta_i$ , will be a vector of orbital elements. This framework could also find applications in the detection of  $\gamma$  ray point sources in complex backgrounds (e.g., [Geringer-Sameth et al., 2015](#)), and is adapted to the retrieval of parametrized periodic signals.

Although our framework is general, we will illustrate our results with the radial velocity technique, whose difficulties motivated our approach. One of the goal of the exoplanet community is to detect numerous Earth-like planets in the habitable zone of Sun-like stars, and to characterize their atmospheres (e.g. [Crossfield, 2015](#); [Quanz et al., 2021](#)). It will be important to detect such planets in the coming years, in particular with radial velocities ([Crass et al., 2021](#)), for future characterisation of their atmosphere, for instance with the instrument PCS [Kasper et al. \(2021\)](#), LUVVOIR<sup>1</sup>, and HabEx<sup>2</sup>. The planet 51 Peg b is a Jupiter-size planet orbiting its star in 4.2 days, which is seven times closer to its host Star than Mercury is to the Sun, and has a RV effect of 55 m/s on its star. The fact that the periods are short means that the signals of different cycles can be stacked on one another, and facilitates the detection. As the field of exoplanets expanded, instruments, observation strategies and data analysis techniques were refined to detect planets of smaller mass and with longer periods. We are however not yet able to detect an Earth twin around a Sun like star: the Earth causes on the Sun a radial velocity signal of 9 cm/s.

The major obstacle to detecting such planets is the presence of stellar noises, which have complex, temporally correlated structures. In radial velocities, they have a signature of at least a few tens of cm/s, and often more (e.g. [Saar and Donahue, 1997](#); [Meunier, Lagrange and Desort, 2010](#); [Meunier, Desort and Lagrange, 2010](#); [Dumusque et al., 2011, 2012](#); [Boisse, Bonfils and Santos, 2012](#); [Dumusque et al., 2017](#); [Cegla, 2019](#); [Collier Cameron et al., 2019](#); [Zhao and Ford, 2022](#)). Instrumental effects also play a role ([Dumusque et al., 2015](#); [Cretignier et al., 2021](#)). Furthermore, due to the observational constraints, the number of samples might be too small for the different sources of signal to be easily separated because of the aliasing phenomenon ([Dawson and Fabrycky, 2010](#); [Hara et al., 2017](#)). Due to these difficulties, it is

---

<sup>1</sup><https://asd.gsfc.nasa.gov/luvvoir/resources/>

<sup>2</sup><https://www.jpl.nasa.gov/habex/documents/>

crucial to ensure that the data are fully exploited, and in particular that the method chosen to assess the statistical significance of planet detections is appropriate.

The number of planets is often decided on the basis of a Bayes factor comparing the  $n + 1$  vs.  $n$  planets hypotheses (e.g. Gregory, 2007; Tuomi and Kotiranta, 2009; Brewer and Donovan, 2015; Díaz et al., 2016; Faria et al., 2016; Ahrer et al., 2021). It is checked that the period has a well defined value with the posterior distribution of the parameters. Alternatively, one can use periodograms associated to a false alarm probability (Baluev, 2008; Zechmeister and Kürster, 2009; Baluev, 2009; Baluev, 2013; Baluev, 2015; Delisle, Hara and Ségransan, 2020), or approximations of Bayesian evidences (Mortier et al., 2015; Feng, Tuomi and Jones, 2017; Delisle et al., 2018) or period search based on sparse recovery (Hara et al., 2017). The orbital elements are refined with a Monte-Carlo Markov chain algorithm (MCMC, Ford, 2005; Foreman-Mackey et al., 2013; Fulton et al., 2018; Eastman et al., 2019). The observational technique that has been the most prolific for the detection of exoplanets is the transit method. The observer measures the light flux of a star as a function of time, and searches for a periodic dip due to a planet passing in between the star and the observer. The detection of signals in transits is usually done with metrics using the signal-to noise ratio (e.g. Kovács, Zucker and Mazeh, 2002; Régulo et al., 2007; Hippke and Heller, 2019) or Bayesian statistics (e.g. Doyle et al., 2000; Defaÿ, Deleuil and Barge, 2001). There is no guarantee that these procedures are optimal for the detection of exoplanets. It is in particular not clear whether the number of planets and their periods should be determined separately. This motivated us to search for the optimal detection criterion, so that subsequent efforts can be focused on improving the models of stellar activity and instrumental effects.

We place our analysis in the Bayesian framework, and as in Müller et al. (2004), we adopt two approaches. First, we compute the maximum utility action, where the objective function to maximise performs a trade-off between false and missed detections. Second, we minimise the expected number of missed detections under a constraint on the expected number of false detections. This framework is intimately linked to Bayesian approaches to false discovery rates (e.g. Efron et al., 2001; Storey, 2003; Müller et al., 2004; Muller, Parmigiani and Rice, 2006; Scott and Berger, 2006; Bogdan, Ghosh and Tokdar, 2008; Guindani, Müller and Zhang, 2009; Stephens, 2016). Our results are also closely linked to the posterior inclusion probability (Barbieri and Berger, 2004).

Our article is organized as follows. In Section 2, we present our theoretical framework. The optimal criterion is searched in the framework of maximum utility in Section 3 and minimum missed detection under constraints on the number of false ones in Section 4. In Section 5, we present what the optimal procedure is, we show an example of application and discuss the relationship of our work with other ones. We conclude in Section 6.

## 2. Formalism.

2.1. *Mathematical framework.* Let us consider a dataset  $y$ , typically a vector, and a likelihood function  $p(y | n, (\theta_i)_{i=1\dots n}, \eta)$  where  $n$  is the number of patterns, where the  $i$ -th pattern is described by parameters  $\theta_i$  all belonging to the same space  $T$ , typically  $T = \mathbb{R}^p$  for some  $p$ . The parameters of the nuisance signals are denoted by  $\eta \in H$  (typically  $H = \mathbb{R}^{p'}$  for some  $p'$ ). For a maximum of  $n_{\max}$  patterns, the space onto which the likelihood is defined is

$$(1) \quad \Theta = H \amalg H \times T \amalg H \times T^2 \amalg \dots \amalg H \times T^{n_{\max}}$$

where  $\amalg$  represents the disjoint union. Here  $n_{\max}$  can be a positive integer or  $+\infty$ . We further assume that there are proper prior distributions for  $n, (\theta_i)_{i=1\dots n}$ , and  $\eta$ . The nuisance effects can be deterministic, such as an intercept or linear trend, or stochastic. In that case  $\eta$  parametrizes the distribution of this effect. For instance, it might include a variance of an additional white, Gaussian noise, or hyperparameters of a correlated stochastic process.

In the present work, we define a detection claim as follows.

DEFINITION 2.1 (Detection claim). We first choose a space  $\mathcal{T}$  that is a set of measurable subspaces of  $T \amalg T^2 \amalg \dots \amalg T^{n_{\max}}$ . Given  $(\Theta_1, \dots, \Theta_n) \in \mathcal{T}$ , a detection claim is denoted by  $a(\Theta_1, \dots, \Theta_n)$  and defined as the event “There are exactly  $n$  patterns, one with parameters in  $\Theta_1$ , one with parameters in  $\Theta_2$ , ..., one with parameters in  $\Theta_n$ ”.

One of the possibilities, if  $T$  is a metric space, is to choose  $\mathcal{T}$  such that the  $\Theta_i$  are closed balls of fixed radius. This conveys the idea that a certain resolution on the parameters is desired.

A detection claim is completely correct if there are  $n$  patterns truly present in the data, whose parameters  $(\theta_i)_{i=1\dots n}$  are such that there exists a permutation of the indices  $\sigma$  with  $\theta_{\sigma(i)} \in \Theta_i$  for all  $i = 1, \dots, n$ . The permutation simply expresses that the order of the  $\Theta_i$ s does not matter. The detection claim can also be partially incorrect. We claim that there is a pattern with parameters in  $\Theta_i$ , if this isn't the case, we count a false detection. Conversely,  $n$  detections are claimed but if in fact there are  $n' > n$  patterns truly present in the data, we count  $n' - n$  missed detections. We use the terminology false and missed detections instead of false positives and false negatives, which are used in the context of discrete hypotheses testing.

In what follows, we need to compute posterior probabilities marginalised on the number of patterns in the data. For instance, the probability of the event “there is one pattern with parameters in  $\Theta_1$ ” is

$$(2) \quad I_{\Theta_1} := \sum_{k \geq 1} p(k | y) \int_{\exists! i, \theta_i \in \Theta_1} p(\theta_1, \dots, \theta_k, \eta | y, k) d\theta_1 \dots d\theta_k d\eta.$$

Some formulae are more conveniently written with the probability not to have a pattern in  $\Theta_1$ . Following [Hara et al. \(2021\)](#) we call it the false inclusion probability (FIP), defined as

$$(3) \quad \text{FIP}_{\Theta_1} := 1 - I_{\Theta_1}.$$

The FIP can be seen as an extension to the non-necessarily linear models considered here of the posterior inclusion probability (PIP), applicable to linear models ([Barbieri and Berger, 2004](#)), although unlike [Barbieri and Berger \(2004\)](#), we are not discussing predictive properties.

In practice, Eq. (2) can be computed with nested sampling algorithms (for our numerical experiments, we use POLYCHORD, [Handley, Hobson and Lasenby, 2015a,b](#)). If one has posterior samples of  $k, \theta, \eta$ , the quantity given in Eq. (2) can simply be estimated as the number of samples such that  $\theta \in \Theta_1$  divided by the total number of samples. Alternatively, one can use the weights of the samples as provided by nested sampling algorithms ([Skilling, 2006](#)).

2.2. *Example.* We give an example of use of the FIP in the context of exoplanet detection. Considering the HARPS radial velocity of the star HD 21693 ([Udry et al., 2019](#)), we want to determine how many planets orbit the star and at which period. We consider the radial velocity time-series  $y$  obtained with the YARARA pipeline ([Cretignier et al., 2021](#)), and model it as a sum of the contribution of  $n$  planets, an intercept, and a Gaussian noise uncorrelated noise. More formally, for the measurement at time  $t$ , the measurement is modelled by

$$(4) \quad y(t) = c_0 + \sum_{j=1}^n f(t, \theta_j) + \epsilon_t$$

$$(5) \quad \epsilon_t \sim G(0, \sigma_t^2 + \sigma_J^2),$$



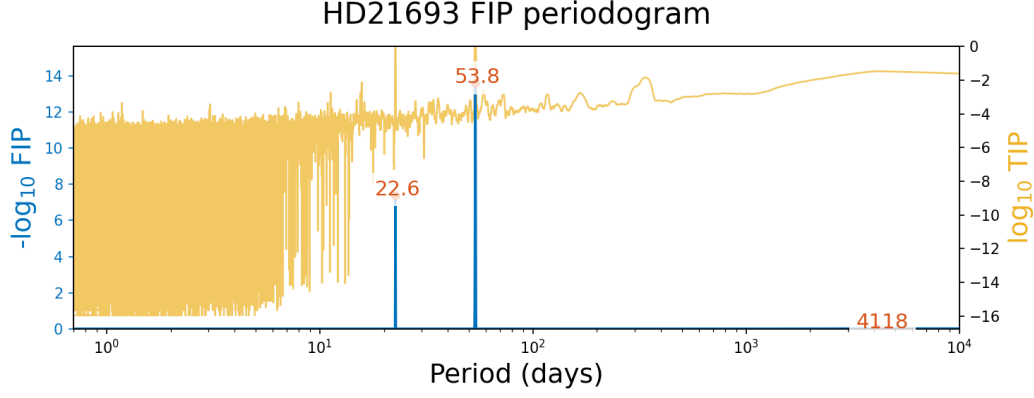


FIG 1. In blue:  $-\log_{10}$  FIP of having a planet with frequency in interval  $[\omega_k - \Delta\omega/2, \omega_k + \Delta\omega/2]$  as a function of  $\omega_k$  for the HARPS data of HD 20003 (Udry et al., 2019) and a maximum of 2 planets. In yellow, we represent the  $TIP = 1 - \text{FIP}$ .

where  $\theta_i$  is the vector of the orbital parameters of planet  $i$  and,  $f$  is as defined in Eq. 1 of (Wright and Howard, 2009), and  $\sigma_t$  is the nominal error bar on the measurement at time  $t$ . The free parameters are  $n, c_0, \sigma_J, (\theta_i)_{i=1..n}$ . We assume that there are at most  $n_{max} = 3$  planets. We fix uninformative priors, which we do not specify for the sake of brevity, as they do not matter for this example.

Following Hara et al. (2021), we consider a grid of frequency intervals with a fixed length. The element  $k$  of the grid is defined as  $[\omega_k - \Delta\omega/2, \omega_k + \Delta\omega/2]$ , where  $\Delta\omega = 2\pi/T_{obs}$ ,  $T_{obs}$  is the total observation time span, and  $\omega_k = k\Delta\omega/N_{oversampling}$ . We take  $N_{oversampling} = 5$ . For each interval in the grid, we compute the marginal probability to have a planet whose frequency lies in the interval, and its FIP as defined in Eq. (3). The FIP as a function of frequency is represented in Fig. 1. The probability that there are no planets with frequencies  $2\pi/53.8 \pm \Delta\omega$  rad/day and  $2\pi/22.67 \pm \Delta\omega$  rad/day period is supported with FIP less than  $10^{-4}$ . The interval with the third highest probability occurs at 4118 days, it has a FIP greater than 90%, and likely stems from low frequency noise.

### 3. Maximum utility.

3.1. *Framework.* We want to minimise both false and missed detections, which is an optimisation problem that we first formalise in the utility framework (von Neumann and Morgenstern, 1947). In this one, a set of possible actions  $\mathcal{A}$  is defined, as well as a utility function  $U$ ,

$$a \in \mathcal{A}, (\theta, \eta) \in \Theta \rightarrow U\{a, (\theta, \eta)\} \in \mathbb{R},$$

quantifying the gain of taking action  $a$  while the true value of the pattern and nuisance parameters is  $\theta$  and  $\eta$ , respectively. The maximum utility action  $a^*$ , if it exists, is defined as

$$(6) \quad a^* = \arg \max_{a \in \mathcal{A}} E_{\theta, \eta} [U\{a, (\theta, \eta)\}] = \arg \max_{a \in \mathcal{A}} \int_{\Theta} U(a, (\theta, \eta)) p(\theta, \eta | y) d\theta d\eta.$$

We must choose the space of actions  $\mathcal{A}$  and the utility function  $U$  for our problem. We choose

$$\mathcal{A} = \{a(\Theta_1, \dots, \Theta_n), (\Theta_i)_{i=1..n} \in \mathcal{T}\}$$

where  $a(\Theta_1, \dots, \Theta_n)$  is given in Definition 2.1. The action is unequivocally defined by the choice of  $(\Theta_i)_{i=1..n} \in \mathcal{T}$ , as a consequence,  $\mathcal{A}$  and  $\mathcal{T}$  can be identified. For our purposes, we

build the utility function as follows. Let us consider that we take the action  $a(\Theta_1, \dots, \Theta_n)$ . We suppose that there are  $n'$  true patterns in the data with pattern parameters  $\theta = (\theta_1, \dots, \theta_{n'})$ . The utility function is defined considering three cases. If  $n = n'$  and for a certain ordering of the  $(\theta_i)_{i=1\dots n}$ ,  $\theta_1 \in \Theta_1, \dots, \theta_n \in \Theta_n$ , then  $U = 0$ . If for a given  $j = 1, \dots, n$  there is no pattern in  $\Theta_j$ , we use a penalization  $-\alpha$  in the utility function, where  $\alpha > 0$ . This event is what we call a false detection. If  $m$  false detections are found, the penalty is  $-m\alpha$ . If  $n$  patterns are claimed, but there are in facts  $n'$  patterns  $n' > n$ , we add to the utility function a term  $-\beta(n' - n)$  where  $\beta > 0$ . By definition of the maximum utility action in Eq. (6), the cost of missed and false detection is weighted by the posterior probability that they happen. We show in Appendix A that the appropriate form for the utility function is

$$(7) \quad E_{\theta, \eta} [U \{a(\Theta_1, \dots, \Theta_n), (\theta, \eta)\}] = -n + \sum_{j=1}^n j I_{A_j} - \gamma \sum_{k=n+1}^{n_{\max}} (k - n) p(k | y),$$

where  $\gamma = \beta/\alpha$ , and  $I_{A_j}$  is the probability that exactly  $j$  detections are correct.

When a pattern detection claim is incorrect, this might also mean that patterns truly present have been missed. In Eq. (7), missing these patterns is penalized only implicitly: getting them right would count as one less false detection. However, we can also explicitly penalize missing patterns. For instance, supposing that there are truly  $n$  patterns and  $n$  patterns claimed, but all are false detections, we now penalize the fact that there are  $n$  missed negatives. In that case, we show in Appendix A that the utility function becomes

$$(8) \quad E_{\theta, \eta} [U \{a, (\theta, \eta)\}] = -n + (1 + \gamma) \sum_{j=1}^n j I_{A_j} - \gamma \sum_{k=1}^{n_{\max}} k p(k | y).$$

In our framework, the candidate  $\Theta_i$  spaces in  $\mathcal{T}$  might have different sizes. If it is the case, the maximisation will favour larger spaces. To prevent this situation, one can either fix the size of the  $\Theta_i$ s as suggested in Section 2, or add a penalisation term to Eq. (7) for the size of the  $\Theta_i$ , for instance, by choosing a certain measure on  $T$  and adding a term  $-\sum_i \mu(\Theta_i)$  to Eq. (7). We leave this latter approach for future work.

**3.2. Patterns with parameters in disjoint regions.** Finding the maximum utility decision consists in finding the maximum of Eq. (7) for  $n = 0..n_{\max}$ , we consider each sub-problem for a fixed  $n$ . If the solution exists, we must then find the optimal  $A_j, j = 1..n$ . As we will see, it is simpler if the  $\Theta_i, i = 1..n$  are disjoint, and this is what we assume in the present section. One possible justification is simply that the physics forbids two patterns to occupy the same  $\Theta_i$ , so that for situations we care about, the maximum is realized for disjoint  $\Theta_i$ s. This is the case whenever we choose the  $\Theta_i$ s as balls of radius  $R$  and the prior  $p(|\theta_i - \theta_j| < 2R, \forall i, j | y)$  is small enough, *a fortiori* when it is vanishing. If the  $\Theta_i$ s are disjoint, we have the following result.

LEMMA 3.1. *Let us consider  $\Theta_1 \in T, \dots, \Theta_n \in T, \forall i_1, i_2 = 1..n, i_1 \neq i_2, \Theta_{i_1} \cap \Theta_{i_2} = \emptyset$ . Then with  $I_{\Theta_i}$  as defined in Eq. (2),*

$$(9) \quad \sum_{j=1}^n j I_{A_j} = \sum_{i=1}^n I_{\Theta_i}$$

The proof, given in Appendix B, simply uses a decomposition of the terms of the left-hand sum. Computing the posterior probability to have a pattern in a space  $\Theta_i$  is simpler than

computing  $A_j$ s, which explore all combination of  $j$  patterns. If Eq. (9) is true, adopting the definition of FIP of Eq. (3), we can re-write Eq. (7) with

$$(10) \quad n - \sum_{j=1}^n j I_{A_j} = n - \sum_{i=1}^n I_{\Theta_i} = \sum_{i=1}^n \text{FIP}_{\Theta_i}.$$

Maximising the utility (Eq. (7)) for a  $n$  pattern model then comes down to solving

$$(P_n) \quad \arg_{\Theta_1 \in T, \dots, \Theta_n \in T, \Theta_i \cap \Theta_j = \emptyset} \min \sum_{i=1}^n \text{FIP}_{\Theta_i} = \arg_{\Theta_1 \in T, \dots, \Theta_n \in T, \Theta_i \cap \Theta_j = \emptyset} \max \sum_{i=1}^n I_{\Theta_i}$$

This raises two questions: whether  $(P_n)$  has a solution, and, if the solution exists, how to find it efficiently. In Appendix C we exhibit some conditions guaranteeing the existence of the solution. In Section 3.3, we establish a few results facilitating the search for a solution.

When searching for periodic signals in time-series, as suggested in Section 2.2 we can choose as  $\mathcal{T}$  a family of disjoint intervals  $[\omega - \Delta\omega/2, \omega + \Delta\omega/2]$  for  $\omega \in [0, \omega_{\max}]$  where  $\Delta\omega$  is fixed. Except for unusual sampling patterns, the frequency resolution is approximately  $\Delta\omega = 2\pi/T_{\text{obs}}$  where  $T_{\text{obs}}$  is the observation time-span. On the other hand, the intrinsic distribution of the signals frequency will typically be such that there cannot be two signals closer than  $\Delta\omega'$ . If the observation time-span is long enough,  $\Delta\omega < \Delta\omega'$ , then one can solve  $(P_n)$  without loss of generality. This remark applies to exoplanets, where planets with orbital periods too close are unstable. There is one caveat to this assumption, which is the potential presence of co-orbital planets (e.g Gascheau, 1843), sharing the same orbit. To address that case, it is possible to either adopt the general formalism of section 3.1, or to further specify the  $\Theta_i$  spaces to ranges of orbital frequencies and phase.

Lemma 3.1 is not true if the  $\Theta_i$ s are allowed to have non empty intersection. This is easily seen for  $n = 2$ , where  $I_{A_1}^1 = I_{\Theta_1 \cup \Theta_2}^1$  which might not be equal to  $I_{\Theta_1}^1 + I_{\Theta_2}^1$  if  $\Theta_1$  and  $\Theta_2$  are not disjoint. To compute Eq. (7) in the general case one can simply use the definition of the  $A_j$  spaces. In the next section, we assume that the  $\Theta_i$ s are disjoint.

**3.3. Searching for the optimum.** Finding the solution to  $(P_n)$  requires in principle to try all combinations of pairwise disjoint  $\Theta_i \subset T$ ,  $i = 1 \dots n$ . However, we can use the solution of  $(P_n)$  to solve  $(P_{n+1})$ . Supposing that Eq.  $(P_n)$  has a solution  $(\Theta_i)_{i=1 \dots n}$ , a natural candidate solution for  $(P_{n+1})$  is to append the space with maximum marginal probability outside of the  $\Theta_i$ s to  $(\Theta_i)_{i=1 \dots n}$ ,

$$(11) \quad \Theta_{n+1}^* = \arg_{\Theta_{n+1} \in T \setminus \bigcup_{i=1}^n \Theta_i^n} \max I_{\Theta_{n+1}}.$$

The following result shows that the solution to  $(P_{n+1})$  is either  $(\Theta_1, \dots, \Theta_n, \Theta_{n+1}^*)$ , or it is to be searched for  $(\Theta_i^{n+1})_{i=1 \dots n+1}$  that all have a non empty intersection with one of the  $(\Theta_i)_{i=1}^n$ .

**LEMMA 3.2.** *Let us suppose that  $(P_n)$  has a solution  $(\Theta_1^n, \dots, \Theta_n^n) \in \mathcal{T}$ . Then the solution to  $(P_{n+1})$  is either  $(\Theta_1^n, \dots, \Theta_n^n, \Theta_{n+1}^*)$  or such that  $\forall i = 1 \dots n+1, \exists j = 1 \dots n, \Theta_i^{n+1} \cap \Theta_j^n \neq \emptyset$ .*

The proof is given in Appendix D. This result motivates the definition of separability, simply expressing the condition under which it can be ensured that the solution to  $(P_{n+1})$  is to append  $\Theta_{n+1}^*$  (Eq. (11)).

**DEFINITION 3.3 (Separability).** We say that a dataset  $y$  verifies patterns separability of order  $n$  if (i) the solution to  $(P_{n-1})$ ,  $\Theta_1^{n-1}, \dots, \Theta_{n-1}^{n-1}$  are pairwise disjoint and (ii) the solution to  $(P_n)$  is  $(\Theta_1^{n-1}, \dots, \Theta_{n-1}^{n-1}, \Theta_n^*)$  as defined in Eq. (11).

If  $T$  is a metric space, we have the following sufficient condition for separability. We denote by  $B(\theta, R)$  a closed balls of centre  $\theta$  and radius  $R$ .

LEMMA 3.4. *Let us suppose that  $\mathcal{T}$  is the set of 0 to  $n_{\max}$  disjoint balls of radius  $R$  and centres  $(\theta_i)_{i=1\dots n}$ . Denoting by  $\Theta^c = \cup_{i=1}^n B(\theta_i, 2R)$ , if  $I_{\Theta^c} < I_{\Theta_{n+1}^*}$ , then the patterns are separable of order  $n + 1$ .*

PROOF.  $\Theta^c$  is the space described by any set of balls of radius  $R$  with a non empty intersection with the  $\Theta_i$ ,  $i = 1\dots n$ . If  $I_{\Theta^c} < I_{\Theta_{n+1}^*}$  there cannot be  $n + 1$  disjoint regions  $(\Theta_i^{n+1})_{i=1\dots n+1}$  with non zero intersection with  $\Theta_i$ ,  $i = 1\dots n$  with  $\sum_{i=1}^{n+1} I_{\Theta_i^{n+1}} \geq I_{\Theta_{n+1}^*} + \sum_{i=1}^n I_{\Theta_i}$ .  $\square$

In the case of exoplanets, where we want to localise the period of planets, Lemma 3.4 means that if the grid of intervals has width  $\Delta\omega$  and the prior excludes two planets being closer than  $2\Delta\omega$ , the separability condition is verified.

#### 4. Minimum missed detections under constraints.

4.1. *Problem formulation.* In section 3, we minimised the number of missed and false detections with a cost function. Alternatively, we can consider the following problem: for an expected number of false positives lower than  $x \in [0, n_{\max}]$ , what is the choice of  $(\Theta_1, \dots, \Theta_n)$  minimising the number of missed detections? This translates to the following optimisation with constraint,

$$(12) \quad \arg \min_{(n, \Theta_1, \dots, \Theta_n)} \sum_{k=n+1}^{n_{\max}} (k - n)p(k | y) \text{ subject to } n - \sum_{j=1}^n jI_{A_j} \leq x.$$

Among the solutions to this problem, we further select the ones that minimize the term  $n - \sum_{j=1}^n jI_{A_j}$ . The rationale is that, for a given value of the objective function, there is no reason to select a solution with a higher expected number of false detection than necessary. Maximising Eq. (7) is similar to a ‘‘Lagrange multipliers’’ version of this constraint. If the  $\Theta_i$  are all assumed to be disjoint, thanks to Lemma 3.1, using Eq. (10), the problem reduces to

$$(13) \quad \arg \min_{(n, \Theta_1, \dots, \Theta_n)} \sum_{k=n+1}^{n_{\max}} (k - n)p(k | y) \text{ subject to } \sum_{i=1}^n \text{FIP}_{\Theta_i} \leq x.$$

where we further select the solution minimising  $\sum_{i=1}^n \text{FIP}_{\Theta_i}$ . A natural question is whether the solutions of (13) obtained as  $x$  skims  $[0, +\infty)$  are the same as the solutions to the maximising utility as  $\gamma$  skims  $[0, +\infty)$ . In the following sections, we show that it is true under certain conditions

4.2. *Link with maximum utility.* In this section, we assume that the  $\Theta_j$  are pairwise disjoint and thus aim at solving problem (13). Let us consider  $\Theta_1, \dots, \Theta_n$  that maximise  $(P_n)$  for a given dataset  $y$ , and define

$$(14) \quad u_n^y := \sum_{i=1}^n \text{FIP}_{\Theta_i}$$

$$(15) \quad v_n^y := \sum_{k=n+1}^{n_{\max}} (k - n)p(k | y).$$

$u_n^y$  is the expected number of false detections and  $v_n^y$  the expected number of missed detections when claiming  $n$  patterns. We then have the following result.

LEMMA 4.1. *For a given posterior probability such that  $(u_{n+1} - u_n)_{n=0..n_{\max}}$  is increasing, we can find an increasing function  $\gamma(x) > 0$  such that the solution of the maximum utility problem (7) solves the constrained problem (12).*

The proof is given in Appendix E. It uses the fact that  $(v_n^y - v_{n+1}^y)_{n=1..n_{\max}}$  is always decreasing, which is evident from the definition of  $v_n^y$ . Furthermore, we can prove the intuitive idea that as the number of claimed patterns increases, so does the number of expected false positives:  $(u_n^y)$  is increasing, as shown in Appendix E. Lemma 4.1 also relies on the fact that  $(u_{n+1} - u_n)_{n=0..n_{\max}}$  is increasing, which is not guaranteed in the general case, but can be ensured under the following condition.

LEMMA 4.2. *If  $\forall n > 0, \exists i_0, \forall j = 1, \dots, n - 1, \Theta_{i_0}^{n+1} \cap \Theta_j^{n-1} = \emptyset$ , the sequence  $(u_{n+1}^y - u_n^y)_{n=1..n_{\max}}$  is increasing.*

The proof is given in Appendix E. If, the condition of Lemma 4.2 is not satisfied one can find a counter example where  $u_{n+1}^y - u_n^y < u_n^y - u_{n-1}^y$  and the equivalence fails. The conditions of Lemma 4.2 are met under the hypothesis of pattern separability, given in Definition 3.3. We then have the following theorem

THEOREM 4.3. *Let us consider a dataset  $y$  and suppose that it verifies pattern separability at all orders  $n = 1..n_{\max}$ , then  $\forall \gamma \in [0, +\infty)$ , there exists a  $x \in [0, +\infty)$  such that (7) and (13) have the same solution.*

PROOF. Under the hypothesis of separability, by lemma 4.2,  $(u_{n+1}^y - u_n^y)_{n=1..n_{\max}}$  is increasing, and by lemma 4.1, we have the desired result.  $\square$

## 5. Discussion.

5.1. *Procedure.* Our initial aim was to find an optimal procedure to determine how many parametric patterns are in the data in the framework described in section 2. To do this, we considered two approaches: the maximum utility decision and minimum expected number of missed detection under a constraint on the expected number of false detections. We have seen in section 4.2 that the two are equivalent, provided a technical condition is satisfied (see Definition 3.3). If it is, then the optimal detection procedure is as follows.

Let us suppose that the signal verifies the separability condition at order  $n + 1$  (see definition 3.3). Then, from Eq. (7) the  $n + 1$  pattern model has a greater utility than the  $n$  pattern model if and only if

$$(16) \quad \text{FIP}_{\Theta_{n+1}^*} \leq \gamma p(k \geq n + 1 | y).$$

where the FIP is defined in Eq. (3) and  $\Theta_{n+1}^*$  is defined in Eq. (11). In the particular case  $\gamma = 1$ , Eq. (16) simply means that the posterior probability to have a  $n + 1$ -th pattern in  $\Theta_{n+1}^*$  should be greater than the probability to have  $n$  patterns or less. It is not surprising that the marginal probability of having a pattern in a certain region appears, since it is the direct probability to have the event of interest and is consistent with a ‘‘Dutch book’’ principle (Ramsey, 1926; De Finetti, 1937).

Eq. (16) means in particular that, for a given  $\gamma$ , the more patterns are claimed, the more stringent the criterion to add a pattern becomes, since the term  $p(k \geq n + 1 | y)$  gets smaller as  $n$  increases. This contrasts with decisions based on a fixed threshold, for instance selecting a model with a Bayes factor greater than 150. However, if we now use the definition of the

utility function (8), the  $n + 1$  pattern model has a greater utility than the  $n$  pattern model if and only if

$$(17) \quad \text{FIP}_{\Theta_{n+1}^*} \leq \frac{\gamma}{\gamma + 1}$$

which expresses the intuitive idea of a bet “ $\gamma$  to one”. If the cost of missing a detection is  $\gamma$  when the cost of a false one is 1, then the FIP of the new signal should be less than  $\gamma/(\gamma + 1)$ .

Unlike Eq. (16), in Eq. (17) the detection threshold is fixed. Typically, we would choose  $\gamma$  small to penalize false detections more than missed ones, thus  $\gamma/(\gamma + 1) \sim \gamma$ . As a consequence, the criterion of Eq. (17) is more stringent than the criterion of Eq. (16). This behaviour is to be expected, because in the second case, we use an extra penalization of missed detection.

As argued in Hara et al. (2021), the FIP has a crucial advantage over the Bayes factor: it is easy to interpret. Indeed, if  $N$  statistically independent detections are made with FIP  $\alpha$ , it means that the number of false detections follows a binomial distribution of parameters  $\alpha$  and  $N$ . The caveat is that in the maximum utility case, one must know the maximum number of patterns possible and be able to compute the Bayesian evidence up to that number, which might be computationally heavy or even intractable. In Hara et al. (2021), to avoid computing Bayesian evidences for high dimensional models, we suggest to add planets in the model until the FIP periodogram (see Section 2.2) does not vary.

*5.2. Applicability.* The formalism adopted requires to make two important choices: the space  $\mathcal{T}$  as in definition 2.1, and whether the separability condition 3.3 applies. If  $T$  is a metric space, we recommend to choose  $\Theta_i$ s as balls of radius  $R$ . If the prior probability to have patterns with parameters  $\theta_1$  and  $\theta_2$  with  $|\theta_1 - \theta_2| < 2R$  is vanishing, then one can search solutions to  $(P_n)$  without loss of generality. The value of  $R$  can always be chosen small enough unless there can be patterns with exactly the same parameters. However, the pattern models typically have an amplitude on which they depend linearly, and the sum of two identical patterns has simply twice the original amplitude. Thanks to Lemma 3.4, if the  $\Theta_i$ s are chosen as balls of fixed radius it is easy to verify that the signal is indeed separable at order  $n + 1$ , and ensure that appending  $\Theta_{n+1}^*$  to the solution of  $(P_n)$  solves  $(P_{n+1})$ . If such simplifications are not possible, one can search to maximise utility in the general case (see Eq. (7) and (8)).

As a remark, our framework is also adapted to problems including both localisation and classification.  $T$  can be chosen as  $X \times C$  where  $X$  is the space of position of the pattern (for instance  $\mathbb{R}^2$ , if we parametrize the center position of the pattern on an image), and  $C$  as a union of  $m$  disjoint subsets (classes)  $C_1, \dots, C_m$ . For a measurable set  $X_0$  of  $X$ , and the parameters of a pattern  $\theta = (x \in X, c \in C)$  we can compute the posterior probability to have a pattern in  $X_0$  of class  $j$ , that is of the event  $x \in X_0, c \in C_j$ . In the context of the search for exoplanets this can be used to disentangle speckles and planets in direct imaging.

*5.3. Example.* To show how the selection criterion (16) performs compared to other significance metrics, we apply it to the detection of sinusoidal signals in unevenly sampled data, where a certain precision on the frequency is desired. We use the simulations of Hara et al. (2021) that emulate a search for exoplanets with radial velocity, the data are thus presented in velocity units (m/s). We describe the simulation briefly below, and refer the reader to Hara et al. (2021) for more details.

We simulate 1000 time-series with 80 time stamps  $t$ , taken as those of first 80 HARPS measurements of HD 69830 (Lovis et al., 2006), which are representative of a typical radial velocity sampling. We inject either no signal, or up to two signals of the form



TABLE 1  
*Priors used to generate and analyse the 1000 systems with circular orbits.*

Parameter	Prior	Values
k	Uniform $[k_{\min}, k_{\max}]$	$k_{\min} = 0, k_{\max} = 2$
A	$G(0, \sigma_A^2)$	$\sigma_A = 1.5$ m/s
B	$G(0, \sigma_B^2)$	$\sigma_B = 1.5$ m/s
C	$G(0, \sigma_C^2)$	$\sigma_C = 1$ m/s
P	log-uniform on $[P_{\min}, P_{\max}]$	$P_{\min} = 1.5, P_{\max} = 100$

$C + \sum_{i=1}^k A_k \cos 2\pi t/P_k + B_k \cos 2\pi t/P_k$ , the distribution of elements  $k, A, B, C, P$  is shown in Table 1. We add a Gaussian white noise according to the nominal error bars, which are typically  $0.54 \pm 0.24$  m/s. We then generated another set of 1000 systems with a lower S/N. The simulation is made with identical parameters except that a correlated Gaussian noise is added. This one has an exponential kernel with a 1 m/s amplitude and a timescale  $\tau = 4$  days. We will refer to these simulations as the high and low signal-to-noise ratio (SNR) simulations.

We analysed the data with different methods, in two steps: one to select the periods of the candidate signals and one to assess their statistical significance. To find the periods, we either use a periodogram [Baluev \(2008\)](#): the period corresponding to the highest peak is subtracted from the data and we compute the periodogram of the residuals, the  $\ell_1$ -periodogram as defined in [Hara et al. \(2017\)](#), based on the basis pursuit algorithm ([Chen, Donoho and Saunders, 1998](#)), or a FIP-periodogram, defined in Section 5.3.

The candidate periods are those of the highest peaks of the different period retrieval methods. We then decide if a planet should be added to the model with different statistical significance metrics: the false alarm probability (FAP) of the periodogram maximum peak ([Baluev, 2008](#)), the Bayes factor (BF) ([Kass and Raftery, 1995](#)), the FIP (see Eq. (3)): a signal is added if its FIP is below a fixed threshold as in (17), or with the criterion (16) for a fixed value of  $\gamma$ . The latter two methods are called ‘‘FIP’’ and ‘‘Maximum utility’’, respectively. We refer to the other methods with the nomenclature ‘‘Period detection + significance metric’’. For instance ‘‘Periodogram + FAP’’ means that we select the highest peak of the periodogram to choose the period and decide its significance based on the FAP. In all cases, the likelihood and priors chosen are consistent with the way the data has been generated.

To evaluate the performance of the different analysis methods, we check whether the frequency of a signal found is less than  $2\pi/T_{\text{obs}}$  away from the true frequency. If not, it is labelled as a false detection. If the claimed planet corresponds to a true planet, we label it as a correct inference and remove its period from the set of true periods, so that a planet cannot be detected twice. If we claim  $n$  planets but there are  $n' > n$  we count  $n' - n$  missed detections. The total number of mistakes is the sum of missed and false detections on the 1000 systems. This definition corresponds to the cost function used in Eq. (7), and we therefore expect that the detection criterion (17) should perform slightly better. In Fig. 2 (a) and (b), we show the total number of mistakes for the high and low SNR simulations, respectively, made with the maximum utility criterion as a function of  $\log_{10} \gamma$ . It appears that the minimum number of mistakes is attained around  $\log_{10} \gamma \sim 0$  that is  $\gamma \sim 1$ , when the missed and false detections are weighted equally.

To compare the different detection methods, we compute the total number of mistakes as a function of the number of false detections, which vary as the detection threshold changes. In Fig. 3 (a) and (b) we show the curves obtained for the high and low SNR simulations, respectively. As expected, the maximum utility criterion outperforms other metrics, notably in the low false positives regime, below  $\sim 10$ , where it leads up to 30% more true detections. It shows very similar performance to simply putting a threshold on the FIP of the signals

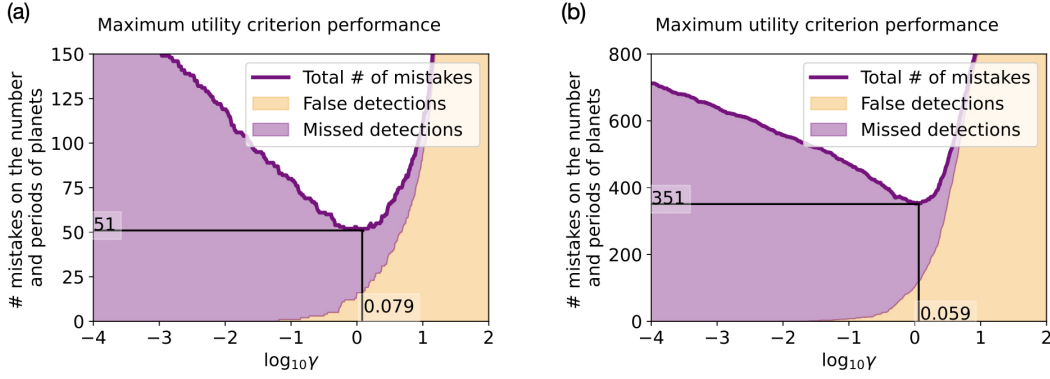


FIG 2. Missed + false detections, in yellow and purple respectively, as a function of the detection threshold,  $\log_{10}\gamma$  where  $\gamma$  is defined in Eq. (16). (a) is obtained on the high SNR simulation and (b) the low SNR simulation. The black plain lines show where the minimum of mistakes is attained.

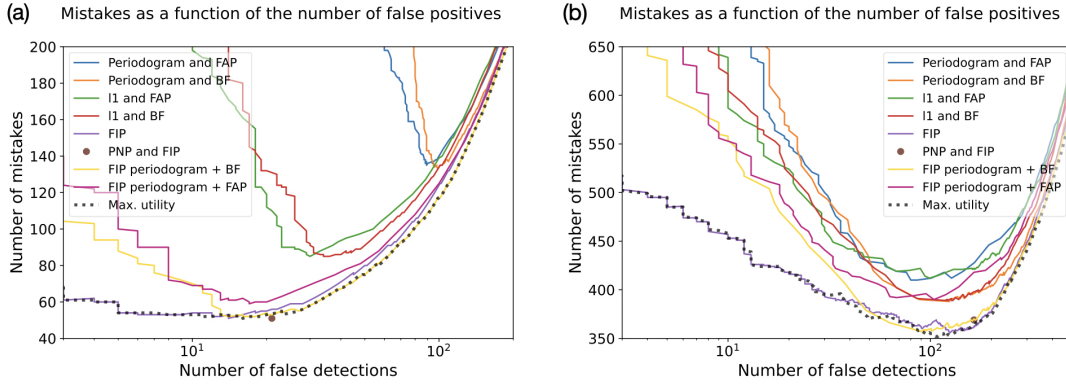


FIG 3. Missed + false detections as a function of the number of false detections for the different analysis methods. The description of the different methods is given in section 5.3. (a) and (b) are obtained on the high and low SNR simulations, respectively.

(plain purple curve), but it appears in Fig. 3 (a) that for a number of false positives greater than 13 the method using the maximum utility consistently outperforms the FIP. In Fig. 3 (a), between  $\sim 60$  and  $\sim 90$  false detections the method “FIP periodogram + BF” shows better performances. This can be due to statistical fluctuations or residual numerical errors.

As mentioned in section 1, our original concern was that deciding on the number of planets with a Bayes factor de-couples the search for the period of the planet and its significance. In our numerical test, all the methods using the FIP periodogram select the candidate period exactly in the same way and differ only in the statistical significance metric. Our results confirm that, indeed, the scale of the significance metric has to be tied to the accuracy desired on the parameters, here on the period. In Hara et al. (2021), we show that this is also the case in practice, through the example of the HARPS radial velocity dataset of HD 10180 (Lovis et al., 2011).

5.4. *Link with other approaches* . In Section 3.1 and 4, we respectively pose the problem in terms of maximisation of utility function and minimum missed detections under constraint on the expected number of false one. Müller et al. (2004) uses the same definition of functions to optimize (they use loss functions instead of utility ones, which is strictly

equivalent) in a different context: gene expression microarrays. In their case, they consider  $n$  different genes which might have an impact or not the result of some experiment, and want to decide for gene  $i$  if it has a significant impact or not. In their parametrization, a variable  $z_i$  plays the role of the ground truth,  $z_i = 0$  means the gene has no impact and  $z_i = 1$ , that it has. The optimal decision rule consists in selecting the  $n^*$  genes with posterior probability of  $z_i = 1$  greater than a certain threshold. They use this result to determine the appropriate sample size. Other works also consider discrete hypotheses, such as (Guindani, Müller and Zhang, 2009). Barbieri and Berger (2004) consider the problem where the data  $y$  are described by a linear model  $y = Ax + \epsilon$ , where each of the components of vector of size  $n$ ,  $x$ , might be zero. They aim at finding the way to select the non zero components to have optimal predictive properties, and find that they must select the components with the probability to be non-zero greater than  $1/2$ .

For our problem, we have to deal with a continuum of possibilities. If we choose the  $\Theta_i$  as balls of fixed radius and center  $\theta$ , our hypotheses are indexed by the continuous variable  $\theta$ . We can however adapt our framework to deal with the cases of Barbieri and Berger (2004); Müller et al. (2004) by selecting  $T$  (see Section 2.1) as a discrete set of indices  $1..n$ , and  $n_{max} = n$ . This means that we aim at selecting  $n^*$  significant variables among  $n$ , and there are at most  $n_{max}$ . We must further impose that for  $i, j = 1..n, i \neq j$ , the prior  $\theta_i \neq \theta_j$ , to forbid to choose twice the same index.

With these choices, the result we would get using the formulation maximum utility function of Eq. (8), would be identical to Müller et al. (2004), but there could be a difference if we used the utility function of Eq. (7). This pertains to the difference between the two utilities in the treatments of false negatives. In Müller et al. (2004), the false negatives are considered as the indices that have wrongly not been selected, and the utility function Eq. (7) does not penalize these situations. In Müller et al. (2004), it is shown that the optimal detection criterion consists in selecting the  $n^*$  genes with a probability  $P(z_i = 1 | y) > c/(c + 1)$  where  $c$  controls the relative cost of false positives and false negatives (in our formalism,  $\gamma = 1/c$ , which is exactly the same as Eq. (17).

In Muller, Parmigiani and Rice (2006), it is shown that the decision rule of Müller et al. (2004) based on a decision-theoretic approach has close links with Bayesian approaches to false discovery rate (FDR) (Efron et al., 2001) (see also Storey (2003); Scott and Berger (2006); Bogdan, Ghosh and Tokdar (2008); Stephens (2016)). The notion of FDR, introduced by Benjamini and Hochberg (1995) aims at controlling the proportion of false positives among the signals whose detection is claimed. As noted in Hara et al. (2021), the FIP provides guarantees on the number of false detections. Indeed, among  $n$  statistically independent claims made with FIP =  $\alpha$ , the number of false ones follows a Bernouilli distributions of parameters  $\alpha$  and  $n$ .

## 6. Conclusion.

6.1. *General case.* Our initial aim was to find an optimal procedure to determine how many parametric patterns are in the data. We modelled the problem in a Bayesian setting, choosing a likelihood of the form  $p(y | n, (\theta_i)_{i=1..n}, \eta)$  where  $y$  is the data,  $n$  the number of patterns,  $(\theta_i)_{i=1..n} \in T^n$  their parameters in a space  $T$ , and  $\eta$  nuisance parameters, and proper priors. We want to determine the number of patterns  $n$  and their elements  $(\theta_i)_{i=1..n}$ . We consider that if a pattern is claimed with parameters in a certain space  $\theta_i \in \Theta_i$ , but there is no such pattern truly in the data, it is a false detection. Conversely, underestimating the number of patterns by  $\Delta n$  consists in  $\Delta n$  missed detections. This formulation requires to choose the candidate regions  $\Theta_i$ . If  $T$  is a metric space, we recommend to choose a set of the closed balls of fixed radius  $R$ , which fixes the resolution desired on the pattern parameters. If

possible, we recommend to choose  $R$  such that two patterns cannot be closer than  $2R$ . In that setting, we can express the optimum decision as a maximum utility problem, expressing a compromise between false and missed detection and parametrized by  $\gamma$ , setting their relative costs. We also explored the formulation where we minimise the expected number of missed detections under a constraint on the expected number of false detections. We found technical conditions under which the two problems are equivalent (see Definition 3.3). The detection conditions (16) and (17) correspond to a slightly different penalization of the missed detection. Depending on the application one might choose one or the other, and select the number of patterns satisfying the condition. If the separability condition is met, for the cost function (8), we find equivalent results as Müller et al. (2004), which considered the discrete case. If the condition is not met, the problem can be solved with a more general formulation (see section 3.1).

6.2. *Exoplanets.* For the detection of exoplanets with radial velocities, this simply means that instead of using the Bayes factor to determine the number of planets, it is more advantageous to proceed as follows. We define  $\Delta\omega = 2\pi/T_{obs}$  where  $T_{obs}$  is the observational time-span, and a grid of tightly spaced frequencies  $\omega_k$  which defines a collection of intervals  $I_k = [\omega_k - \Delta\omega/2, \omega_k + \Delta\omega/2]$ . One then simply has to compute the posterior probability to have a planet with frequency in  $I_k$  (TIP) or the FIP = 1-TIP. The next step is to select the maximum number  $n^*$  of disjoint intervals with a FIP satisfying either the condition (16) or see Eq. (17), which correspond to slightly different penalization of false negatives. We recommend the latter for simplicity, which is simply taking the intervals with FIP lower than a certain threshold (see Hara et al. (2021) for a practical example).

For other observational technique the procedure is the same. If a correct detection is defined as one of the parameters being in a certain region, one must compute the posterior probability to have a planet with parameters in this region marginalised on the number of planets. The major issue for transits, imaging and microlensing will be the computational tractability, since the datasets are typically much more voluminous.

6.3. *Future work.* From a theoretical perspective, the next step will be to determine an analytical approximation of the minimum expected number of missed detections under a constraint on expected number of false detections, as a function of the prior distribution of parameters and the likelihood. This way, it will be possible to predict the optimal capabilities of a survey operating at a certain precision, if the data model is perfectly known. Furthermore, we can explore the robustness of our results to errors in the model. This has been done through simulations in Hara et al. (2021) but could be also addressed analytically as in Risser, Paciorek and Stone (2019).

We tested the improvements in terms of false and missed detection of the new detection criterion for radial velocities. It will also be interesting to test the improvements on the detection capabilities of other types of observational techniques (transits, astrometry, etc).

**Acknowledgements.** N. C. Hara thanks Gwenaël Boué for his insightful remarks and Roberto Trotta for his suggestions. N. C. Hara and J.-B. Delisle acknowledge the financial support of the National Centre for Competence in Research PlanetS of the Swiss National Science Foundation (SNSF). T. de Poyferré acknowledges support by the NSF under Grant No.DMS-1928930 while participating in a program hosted by MSRI in Berkeley, Ca, during Spring 2021.

## REFERENCES

- AHRER, E., QUELOZ, D., RAJPAUL, V. M., SÉGRANSAN, D., BOUCHY, F., HALL, R., HANDLEY, W., LOVIS, C., MAYOR, M., MORTIER, A., PEPE, F., THOMPSON, S., UDRY, S. and UNGER, N. (2021). The HARPS search for southern extra-solar planets - XLV. Two Neptune mass planets orbiting HD 13808: a study of stellar activity modelling's impact on planet detection. *MNRAS* **503** 1248-1263.
- BALUEV, R. V. (2008). Assessing the statistical significance of periodogram peaks. *MNRAS* **385** 1279-1285.
- BALUEV, R. V. (2009). Accounting for velocity jitter in planet search surveys. *MNRAS* **393** 969-978.
- BALUEV, R. V. (2013). Detecting multiple periodicities in observational data with the multifrequency periodogram – I. Analytic assessment of the statistical significance. *Monthly Notices of the Royal Astronomical Society* **436** 807-818.
- BALUEV, R. V. (2015). Keplerian periodogram for Doppler exoplanet detection: optimized computation and analytic significance thresholds. *MNRAS* **446** 1478-1492.
- BARBIERI, M. M. and BERGER, J. O. (2004). Optimal Predictive Model Selection. *The Annals of Statistics* **32** 870–897.
- BENJAMINI, Y. and HOCHBERG, Y. (1995). Controlling the False Discovery Rate: A Practical and Powerful Approach to Multiple Testing. *Journal of the Royal Statistical Society. Series B (Methodological)* **57** 289–300.
- BOGDAN, M., GHOSH, J. K. and TOKDAR, S. T. (2008). A comparison of the Benjamini-Hochberg procedure with some Bayesian rules for multiple testing. In *Beyond parametrics in interdisciplinary research: Festschrift in honor of Professor Pranab K. Sen* 211–230. Institute of Mathematical Statistics.
- BOISSE, I., BONFILS, X. and SANTOS, N. C. (2012). SOAP. A tool for the fast computation of photometry and radial velocity induced by stellar spots. *A&A* **545** A109.
- BREWER, B. J. and DONOVAN, C. P. (2015). Fast Bayesian inference for exoplanet discovery in radial velocity data. *MNRAS* **448** 3206-3214.
- CEGLA, H. (2019). The Impact of Stellar Surface Magnetoconvection and Oscillations on the Detection of Temperate, Earth-Mass Planets Around Sun-Like Stars. *Geosciences* **9** 114.
- CHEN, S. S., DONOHO, D. L. and SAUNDERS, M. A. (1998). Atomic decomposition by basis pursuit. *SIAM JOURNAL ON SCIENTIFIC COMPUTING* **20** 33–61.
- COLLIER CAMERON, A., MORTIER, A., PHILLIPS, D., DUMUSQUE, X., HAYWOOD, R. D., LANGELLIER, N., WATSON, C. A., CEGLA, H. M., COSTES, J., CHARBONNEAU, D., COFFINET, A., LATHAM, D. W., LOPEZ-MORALES, M., MALAVOLTA, L., MALDONADO, J., MICELA, G., MILBOURNE, T., MOLINARI, E., SAAR, S. H., THOMPSON, S., BUCHSCHACHER, N., CECCONI, M., COSENTINO, R., GHEDINA, A., GLENDAY, A., GONZALEZ, M., LI, C. H., LODI, M., LOVIS, C., PEPE, F., PORETTI, E., RICE, K., SASSELOV, D., SOZZETTI, A., SZENTGYORGYI, A., UDRY, S. and WALSWORTH, R. (2019). Three years of Sun-as-a-star radial-velocity observations on the approach to solar minimum. *MNRAS* **487** 1082-1100.
- CRASS, J., GAUDI, B. S., LEIFER, S., BEICHMAN, C., BENDER, C., BLACKWOOD, G., BURT, J. A., CALLAS, J. L., CEGLA, H. M., DIDDAMS, S. A., DUMUSQUE, X., EASTMAN, J. D., FORD, E. B., FULTON, B., GIBSON, R., HALVERSON, S., HAYWOOD, R. D., HEARTY, F., HOWARD, A. W., LATHAM, D. W., LÖHNER-BÖTTCHER, J., MAMAJEK, E. E., MORTIER, A., NEWMAN, P., PLAVCHAN, P., QUIRRENBACH, A., REINERS, A., ROBERTSON, P., ROY, A., SCHWAB, C., SEIFAHRT, A., SZENTGYORGYI, A., TERRIEN, R., TESKE, J. K., THOMPSON, S. and VASISHT, G. (2021). Extreme Precision Radial Velocity Working Group Final Report. *arXiv e-prints* arXiv:2107.14291.
- CRETIGNIER, M., DUMUSQUE, X., HARA, N. C. and PEPE, F. (2021). YARARA: Significant improvement in RV precision through post-processing of spectral time series. *A&A* **653** A43.
- CROSSFIELD, I. J. M. (2015). Observations of Exoplanet Atmospheres. *ApSP* **127** 941.
- DAWSON, R. I. and FABRYCKY, D. C. (2010). Radial Velocity Planets De-aliased: A New, Short Period for Super-Earth 55 Cnc e. *ApJ* **722** 937-953.
- DE FINETTI, B. (1937). Foresight: Its logical laws, its subjective sources. In *Breakthroughs in statistics* 134–174. Springer.
- DEFAÏ, C., DELEUIL, M. and BARGE, P. (2001). A Bayesian method for the detection of planetary transits. *A&A* **365** 330-340.
- DELISLE, J. B., HARA, N. and SÉGRANSAN, D. (2020). Efficient modeling of correlated noise. I. Statistical significance of periodogram peaks. *A&A* **635** A83.
- DELISLE, J. B., SÉGRANSAN, D., DUMUSQUE, X., DIAZ, R. F., BOUCHY, F., LOVIS, C., PEPE, F., UDRY, S., ALONSO, R., BENZ, W., COFFINET, A., COLLIER CAMERON, A., DELEUIL, M., FIGUEIRA, P., GILLON, M., LO CURTO, G., MAYOR, M., MORDASINI, C., MOTALEBI, F., MOUTOU, C., POLLACCO, D., POMPEI, E., QUELOZ, D., SANTOS, N. C. and WYTENBACH, A. (2018). The HARPS search for southern extra-solar planets. XLIII. A compact system of four super-Earth planets orbiting HD 215152. *A&A* **614** A133.

- DÍAZ, R. F., SÉGRANSAN, D., UDRY, S., LOVIS, C., PEPE, F., DUMUSQUE, X., MARMIER, M., ALONSO, R., BENZ, W., BOUCHY, F., COFFINET, A., COLLIER CAMERON, A., DELEUIL, M., FIGUEIRA, P., GILLON, M., LO CURTO, G., MAYOR, M., MORDASINI, C., MOTALEBI, F., MOUTOU, C., POLLACCO, D., POMPEI, E., QUELOZ, D., SANTOS, N. and WYTENBACH, A. (2016). The HARPS search for southern extra-solar planets. XXXVIII. Bayesian re-analysis of three systems. New super-Earths, unconfirmed signals, and magnetic cycles. *A&A* **585** A134.
- DOYLE, L. R., DEEG, H. J., KOZHEVNIKOV, V. P., OETIKER, B., MARTÍN, E. L., BLUE, J. E., ROTTLER, L., STONE, R. P. S., NINKOV, Z., JENKINS, J. M., SCHNEIDER, J., DUNHAM, E. W., DOYLE, M. F. and PALEOLOGOU, E. (2000). Observational Limits on Terrestrial-sized Inner Planets around the CM Draconis System Using the Photometric Transit Method with a Matched-Filter Algorithm. *ApJ* **535** 338-349.
- DUMUSQUE, X., UDRY, S., LOVIS, C., SANTOS, N. C. and MONTEIRO, M. J. P. F. G. (2011). Planetary detection limits taking into account stellar noise. I. Observational strategies to reduce stellar oscillation and granulation effects. *A&A* **525** A140.
- DUMUSQUE, X., PEPE, F., LOVIS, C., SÉGRANSAN, D., SAHLMANN, J., BENZ, W., BOUCHY, F., MAYOR, M., QUELOZ, D., SANTOS, N. and UDRY, S. (2012). An Earth-mass planet orbiting  $\alpha$  Centauri B. *Nature* **491** 207-211.
- DUMUSQUE, X., PEPE, F., LOVIS, C. and LATHAM, D. W. (2015). Characterization of a Spurious One-year Signal in HARPS Data. *ApJ* **808** 171.
- DUMUSQUE, X., BORSA, F., DAMASSO, M., DÍAZ, R. F., GREGORY, P. C., HARA, N. C., HATZES, A., RAJPAUL, V., TUOMI, M., AIGRAIN, S., ANGLADA-ESCUDE, G., BONOMO, A. S., BOUÉ, G., DAUVERGNE, F., FRUSTAGLI, G., GIACOBBE, P., HAYWOOD, R. D., JONES, H. R. A., LASKAR, J., PINAMONTI, M., PORETTI, E., RAINER, M., SÉGRANSAN, D., SOZZETTI, A. and UDRY, S. (2017). Radial-velocity fitting challenge. II. First results of the analysis of the data set. *A&A* **598** A133.
- EASTMAN, J. D., RODRIGUEZ, J. E., AGOL, E., STASSUN, K. G., BEATTY, T. G., VANDERBURG, A., GAUDI, B. S., COLLINS, K. A. and LUGER, R. (2019). EXOFASTv2: A public, generalized, publication-quality exoplanet modeling code. *arXiv e-prints* arXiv:1907.09480.
- EFRON, B., TIBSHIRANI, R., STOREY, J. D. and TUSHER, V. (2001). Empirical Bayes analysis of a microarray experiment. *Journal of the American statistical association* **96** 1151–1160.
- FARIA, J. P., HAYWOOD, R. D., BREWER, B. J., FIGUEIRA, P., OSHAGH, M., SANterne, A. and SANTOS, N. C. (2016). Uncovering the planets and stellar activity of CoRoT-7 using only radial velocities. *A&A* **588** A31.
- FENG, F., TUOMI, M. and JONES, H. R. A. (2017). Agatha: disentangling periodic signals from correlated noise in a periodogram framework. *MNRAS* **470** 4794-4814.
- FORD, E. B. (2005). Quantifying the Uncertainty in the Orbits of Extrasolar Planets. *AJ* **129** 1706-1717.
- FOREMAN-MACKEY, D., HOGG, D. W., LANG, D. and GOODMAN, J. (2013). emcee: The MCMC Hammer. *ApSP* **125** 306.
- FULTON, B. J., PETIGURA, E. A., BLUNT, S. and SINUKOFF, E. (2018). RadVel: The Radial Velocity Modeling Toolkit. *ApSP* **130** 044504.
- GASCHEAU, M. (1843). Examen d'une classe d'équations différentielles et application à un cas particulier du problème des trois corps. *Comptes Rendus* **16** 393.
- GERINGER-SAMETH, A., WALKER, M. G., KOUSHIAPPAS, S. M., KOPOSOV, S. E., BELOKUROV, V., TORREALBA, G. and EVANS, N. W. (2015). Indication of Gamma-Ray Emission from the Newly Discovered Dwarf Galaxy Reticulum II. *PRL* **115** 081101.
- GREGORY, P. C. (2007). A Bayesian periodogram finds evidence for three planets in HD 11964. *MNRAS* **381** 1607-1616.
- GUINDANI, M., MÜLLER, P. and ZHANG, S. (2009). A Bayesian discovery procedure. *Journal of the Royal Statistical Society: Series B (Statistical Methodology)* **71** 905–925.
- HANDLEY, W. J., HOBSON, M. P. and LASENBY, A. N. (2015a). polychord: nested sampling for cosmology. *MNRAS* **450** L61-L65.
- HANDLEY, W. J., HOBSON, M. P. and LASENBY, A. N. (2015b). POLYCHORD: next-generation nested sampling. *MNRAS* **453** 4384-4398.
- HARA, N. C., BOUÉ, G., LASKAR, J. and CORREIA, A. C. M. (2017). Radial velocity data analysis with compressed sensing techniques. *MNRAS* **464** 1220-1246.
- HARA, N. C., UNGER, N., DELISLE, J.-B., DÍAZ, R. and SÉGRANSAN, D. (2021). Improving exoplanet detection capabilities with the false inclusion probability. Comparison with other detection criteria in the context of radial velocities. *arXiv e-prints* arXiv:2105.06995.
- HIPPKE, M. and HELLER, R. (2019). Optimized transit detection algorithm to search for periodic transits of small planets. *A&A* **623** A39.



- KASPER, M., CERPA URRA, N., PATHAK, P., BONSE, M., NOUSIAINEN, J., ENGLER, B., TAÏSSIR HERITIER, C., KAMMERER, J., LEVERATTO, S., RAJANI, C., BRISTOW, P., LE LOUARN, M., MADEC, P.-Y., STRÖBELE, S., VERINAUD, C., GLAUSER, A., QUANZ, S. P., HELIN, T., KELLER, C., SNIK, F., BOCCALETTI, A., CHAUVIN, G., MOUILLET, D., KULCSÁR, C. and RAYNAUD, H.-F. (2021). PCS – A Roadmap for Exoearth Imaging with the ELT. *arXiv e-prints* arXiv:2103.11196.
- KASS, R. E. and RAFTERY, A. E. (1995). Bayes Factors. *Journal of the American Statistical Association* **90** 773-795.
- KOVÁCS, G., ZUCKER, S. and MAZEH, T. (2002). A box-fitting algorithm in the search for periodic transits. *A&A* **391** 369-377.
- LOVIS, C., MAYOR, M., PEPE, F., ALIBERT, Y., BENZ, W., BOUCHY, F., CORREIA, A. C. M., LASKAR, J., MORDASINI, C., QUELOZ, D., SANTOS, N. C., UDRY, S., BERTAUX, J.-L. and SIVAN, J.-P. (2006). An extrasolar planetary system with three Neptune-mass planets. *Nature* **441** 305-309.
- LOVIS, C., SÉGRANSAN, D., MAYOR, M., UDRY, S., BENZ, W., BERTAUX, J. L., BOUCHY, F., CORREIA, A. C. M., LASKAR, J., LO CURTO, G., MORDASINI, C., PEPE, F., QUELOZ, D. and SANTOS, N. C. (2011). The HARPS search for southern extra-solar planets. XXVIII. Up to seven planets orbiting HD 10180: probing the architecture of low-mass planetary systems. *A&A* **528** A112.
- MAYOR, M. and QUELOZ, D. (1995). A Jupiter-mass companion to a solar-type star. *Nature* **378** 355-359.
- MEUNIER, N., DESORT, M. and LAGRANGE, A. M. (2010). Using the Sun to estimate Earth-like planets detection capabilities . II. Impact of plages. *A&A* **512** A39.
- MEUNIER, N., LAGRANGE, A. M. and DESORT, M. (2010). Reconstructing the solar integrated radial velocity using MDI/SOHO. *A&A* **519** A66.
- MORTIER, A., FARIA, J. P., CORREIA, C. M., SANTERNE, A. and SANTOS, N. C. (2015). BGLS: A Bayesian formalism for the generalised Lomb-Scargle periodogram. *A&A* **573** A101.
- MULLER, P., PARMIGIANI, G. and RICE, K. (2006). FDR and Bayesian multiple comparisons rules.
- MÜLLER, P., PARMIGIANI, G., ROBERT, C. and ROUSSEAU, J. (2004). Optimal Sample Size for Multiple Testing. *Journal of the American Statistical Association* **99** 990-1001.
- PERRYMAN, M. (2018). *The Exoplanet Handbook*.
- QUANZ, S. P., OTTIGER, M., FONTANET, E., KAMMERER, J., MENTI, F., DANNERT, F., GHEORGHE, A., ABSIL, O., AIRAPETIAN, V. S., ALEI, E., ALLART, R., ANGERHAUSEN, D., BLUMENTHAL, S., BUCHHAVE, L. A., CABRERA, J., CARRIÓN-GONZÁLEZ, Ó., CHAUVIN, G., DANCHI, W. C., DANDUMONT, C., DEFRÈRE, D., DORN, C., EHRENREICH, D., ERTTEL, S., FRIDLUND, M., GARCÍA MUÑOZ, A., GASCÓN, C., GIRARD, J. H., GLAUSER, A., GRENFELL, J. L., GUIDI, G., HAGELBERG, J., HELLED, R., IRELAND, M. J., KOPPARAPU, R. K., KORTH, J., KOZAKIS, T., KRAUS, S., LÉGER, A., LEEDIÄRV, L., LICHTENBERG, T., LILLO-BOX, J., LINZ, H., LISEAU, R., LOICQ, J., MAHENDRA, V., MALBET, F., MATHEW, J., MENNESSON, B., MEYER, M. R., MISHRA, L., MOLAVERDIKHANI, K., NOACK, L., OZA, A. V., PALLÉ, E., PARVIAINEN, H., QUIRRENBACH, A., RAUER, H., RIBAS, I., RICE, M., ROMAGNOLO, A., RUGHEIMER, S., SCHWIETERMAN, E. W., SERABYN, E., SHARMA, S., STASSUN, K. G., SZULÁGYI, J., WANG, H. S., WUNDERLICH, F., WYATT, M. C. and THE LIFE COLLABORATION (2021). Large Interferometer For Exoplanets (LIFE): I. Improved exoplanet detection yield estimates for a large mid-infrared space-interferometer mission. *arXiv e-prints* arXiv:2101.07500.
- RAMSEY, P. F. (1926). *Truth and Probability In Studies in Subjective Probability*. Huntington, NY: Robert E. Kreiger Publishing Co.
- RÉGULO, C., ALMENARA, J. M., ALONSO, R., DEEG, H. and ROCA CORTÉS, T. (2007). TRUFAS, a wavelet-based algorithm for the rapid detection of planetary transits. *A&A* **467** 1345-1352.
- RISSER, M. D., PACIOREK, C. J. and STONE, D. A. (2019). Spatially Dependent Multiple Testing Under Model Misspecification, With Application to Detection of Anthropogenic Influence on Extreme Climate Events. *Journal of the American Statistical Association* **114** 61-78.
- SAAR, S. H. and DONAHUE, R. A. (1997). Activity-Related Radial Velocity Variation in Cool Stars. *ApJ* **485** 319-327.
- SCOTT, J. G. and BERGER, J. O. (2006). An exploration of aspects of Bayesian multiple testing. *Journal of Statistical Planning and Inference* **136** 2144-2162. In Memory of Dr. Shanti Swarup Gupta.
- SKILLING, J. (2006). Nested sampling for general Bayesian computation. *Bayesian Analysis* **1** 833 – 859.
- STEPHENS, M. (2016). False discovery rates: a new deal. *Biostatistics* **18** 275-294.
- STOREY, J. D. (2003). The positive false discovery rate: a Bayesian interpretation and the q-value. *The Annals of Statistics* **31** 2013–2035.
- TUOMI, M. and KOTIRANTA, S. (2009). Bayesian analysis of the radial velocities of HD 11506 reveals another planetary companion. *A&A* **496** L13-L16.
- UDRY, S., DUMUSQUE, X., LOVIS, C., SÉGRANSAN, D., DIAZ, R. F., BENZ, W., BOUCHY, F., COFFINET, A., LO CURTO, G., MAYOR, M., MORDASINI, C., MOTALEBI, F., PEPE, F., QUELOZ, D., SANTOS, N. C.,

- WYTENBACH, A., ALONSO, R., COLLIER CAMERON, A., DELEUIL, M., FIGUEIRA, P., GILLON, M., MOUTOU, C., POLLACCO, D. and POMPEI, E. (2019). The HARPS search for southern extra-solar planets. XLIV. Eight HARPS multi-planet systems hosting 20 super-Earth and Neptune-mass companions. *A&A* **622** A37.
- VON NEUMANN, J. and MORGENSTERN, O. (1947). *Theory of games and economic behavior*. Princeton University Press.
- WOLSZCZAN, A. and FRAIL, D. A. (1992). A planetary system around the millisecond pulsar PSR1257 + 12. *Nature* **355** 145-147.
- WRIGHT, J. T. and HOWARD, A. W. (2009). Efficient Fitting of Multiplanet Keplerian Models to Radial Velocity and Astrometry Data. *ApJS* **182** 205-215.
- ZECHMEISTER, M. and KÜRSTER, M. (2009). The generalised Lomb-Scargle periodogram. A new formalism for the floating-mean and Keplerian periodograms. *A&A* **496** 577-584.
- ZHAO, J. and FORD, E. B. (2022). FIESTA II. Disentangling stellar and instrumental variability from exoplanetary Doppler shifts in Fourier domain. *arXiv e-prints* arXiv:2201.03780.

## APPENDIX A: EXPRESSION OF THE UTILITY FUNCTION

In this appendix, we show how to obtain the expression of the utility function (7). We make a detection claim as in Definition 2.1), and penalise false and missed detections as described in Section 3.1. Let us first compute the utility function for the claim “there is no pattern”, denoted by  $a_0$ .

$$(18) \quad E_{\eta}\{U(a_0, \eta)\} = 0 \times p(0 | y) - \beta \sum_{k=1}^{n_{max}} kp(k | y).$$

If in fact there are  $k$  patterns, we “pay”  $k\beta$ , hence the  $-\beta \sum_{k=1}^n kp(k | y)$  term, where  $p(k | y)$  the posterior probability of having  $k$  patterns.

When claiming the detection of  $n > 0$  patterns with parameters in  $\Theta_i$ ,  $i = 1..n$ , the  $\Theta_i$ s can be considered as  $n$  “boxes”. We want to evaluate the utility of this claim if the true patterns have parameters  $\theta_1, \dots, \theta_k$ , where  $k$  might be different from  $n$ . We consider ways to put the  $\theta_i$  in the boxes such that each  $\theta_i$  can go into only one “box”. Thus, if one of the  $\theta_i$  is such that  $\theta_i$  belongs to several  $\Theta_j$ , we consider that only one pattern has been found. We denote by  $m$  the maximum number of different  $\theta_i$ s that we can put in a  $\Theta_i$ . We denote by  $A_m^k$  the region of parameter space with  $k$  patterns such that there is exactly one pattern in each of the  $\Theta_i$ ,  $i = 1..m$ ,  $m \leq n$ .

$$(19) \quad E_{\theta, \eta}[U\{a, (\theta, \eta)\}] = -n\alpha p(0 | y)$$

$$(20) \quad + [-(n-1)\alpha I_{A_1^1} - n\alpha(1 - I_{A_1^1})] p(1 | y)$$

$$(21) \quad + [-(n-2)\alpha I_{A_2^2} - (n-1)\alpha I_{A_1^2} - n\alpha(1 - I_{A_1^2} - I_{A_2^2})] p(2 | y)$$

$$(22) \quad \vdots$$

$$(23) \quad + \left[ \sum_{i=1}^n -(n-i)\alpha I_{A_i^n} - n\alpha \left( 1 - \sum_{i=1}^n I_{A_i^n} \right) \right] p(n | y)$$

$$(24) \quad + \left[ \sum_{i=1}^n -(n-i)\alpha I_{A_i^{n+1}} - n\alpha \left( 1 - \sum_{i=1}^n I_{A_i^{n+1}} \right) - \beta \right] p(n+1 | y)$$

$$(25) \quad \vdots$$

$$(26) \quad + \left[ \sum_{i=1}^n -(n-i)\alpha I_{A_i^n} - n\alpha \left( 1 - \sum_{i=1}^n I_{A_i^{n_{max}}} \right) - (n_{max} - n)\beta \right] p(n_{max} | y)$$

Re-arranging the terms, we have

$$(27) \quad E_{\theta,\eta}[U\{a, (\theta, \eta)\}] = -n\alpha + \alpha \sum_{i=1}^n iI_{A_i} - \beta \sum_{k=n+1}^{n_{max}} (k-n)p(k|y)$$

Assuming that  $\alpha \neq 0$  (or equivalently  $\alpha > 0$ , since  $\alpha$  is non negative), we can divide Eq. (27) by  $\alpha$ . Denoting by  $\gamma = \beta/\alpha$ , without loss of generality we can maximize

$$(28) \quad E_{\theta,\eta}[U\{a(\Theta_1, \dots, \Theta_n), (\theta, \eta)\}] = -n + \sum_{j=1}^n jI_{A_j} - \gamma \sum_{k=n+1}^{n_{max}} (k-n)p(k|y).$$

Alternatively, we can further penalize the missed detections. If  $k$  planets are truly present in the data,  $n$  detections are claimed but only  $i$  are correct, it means that the true detections of  $\max(k, n) - i$  are missed. We can penalize this situation by adding a term  $-\beta(\max(k, n) - i)$  whenever it happens. The expression of the utility function is now

$$(29)$$

$$E_{\theta,\eta}[U\{a, (\theta, \eta)\}] = -n\alpha p(0|y)$$

$$(30)$$

$$+ [-(n-1)\alpha I_{A_1} - (n\alpha + \beta)(1 - I_{A_1})] p(1|y)$$

$$(31)$$

$$+ [-(n-2)\alpha I_{A_2} - ((n-1)\alpha + \beta)I_{A_1} - (n\alpha + 2\beta)(1 - I_{A_1} - I_{A_2})] p(2|y)$$

$$(32)$$

⋮

$$(33)$$

$$+ \left[ \sum_{i=1}^k (-(n-i)\alpha - (k-i)\beta)I_{A_i^k} - (n\alpha + k\beta) \left( 1 - \sum_{i=1}^k I_{A_i^k} \right) \right] p(k|y)$$

$$(34)$$

⋮

$$(35)$$

$$+ \left[ \sum_{i=1}^n -(n-i)(\alpha + \beta)I_{A_i^n} - n(\alpha + \beta) \left( 1 - \sum_{i=1}^n I_{A_i^n} \right) \right] p(n|y)$$

$$(36)$$

$$+ \left[ \sum_{i=1}^n -(n-i)(\alpha + \beta)I_{A_i^{n+1}} - n(\alpha + \beta) \left( 1 - \sum_{i=1}^n I_{A_i^{n+1}} \right) - \beta \right] p(n+1|y)$$

$$(37)$$

⋮

$$(38)$$

$$+ \left[ \sum_{i=1}^n -(n-i)(\alpha + \beta)I_{A_i^n} - n(\alpha + \beta) \left( 1 - \sum_{i=1}^n I_{A_i^{n_{max}}} \right) - (n_{max} - n)\beta \right] p(n_{max}|y)$$

Re-arranging the terms, we have

$$(39) \quad E_{\theta, \eta} [U \{a, (\theta, \eta)\}] = -n\alpha + (\alpha + \beta) \sum_{i=1}^n i I_{A_i} - \beta \sum_{k=1}^{n_{max}} kp(k | y)$$

Again, re-normalizing by  $\alpha > 0$

$$(40) \quad E_{\theta, \eta} [U \{a, (\theta, \eta)\}] = -n + (1 + \gamma) \sum_{i=1}^n i I_{A_i} - \gamma \sum_{k=1}^{n_{max}} kp(k | y).$$

The sum on the right is simply the expectancy of  $k$  and does not depend on the number of planets.

## APPENDIX B: PROOF OF LEMMA 1

LEMMA B.1. *Let us consider  $\Theta_1 \in T, \dots, \Theta_n \in T, \forall i_1, i_2 = 1 \dots n, i_1 \neq i_2, \Theta_{i_1} \cap \Theta_{i_2} = \emptyset$ . Denoting by  $A_i$  the subset of  $\Theta$  such that there are exactly  $i$  patterns in  $\Theta_1, \dots, \Theta_n$ , then*

$$(41) \quad \sum_{j=1}^n j I_{A_j} = \sum_{i=1}^n I_{\Theta_i}$$

where  $I_{\Theta_i}$  is defined in Eq. 2

We first begin with a technical remark.

FACT. Since all patterns are interchangeable in the model, the ordering chosen between them is of no consequence. The detection claims are invariant by relabeling of the parameters, between different factors of  $T$ , i.e. having exactly one pattern in  $\Theta_1, \dots$  exactly one in  $\Theta_n$  is equivalent to having exactly one pattern in  $\Theta_{\sigma(1)}, \dots$  exactly one in  $\Theta_{\sigma(n)}$  for any permutation  $\sigma$  of the  $n$  labels.

PROOF. Let us denote by  $\Theta_1 \wedge \Theta_2 \wedge \dots \wedge \Theta_j \setminus \Theta_{j+1}, \dots, \Theta_n$  regions of  $\Theta$  such that  $j$  patterns are in  $\Theta_1, \Theta_2, \dots, \Theta_j$  and no patterns are in  $\Theta_{j+1}, \dots, \Theta_n$ . Then, since the  $\Theta_i$  are disjoint, we can decompose  $I_{\Theta_i}$  as a sum of posterior mass over regions that have a pattern in  $\Theta_i$  but not other pattern in one of the  $\Theta_j, j \neq i$ , regions that have a pattern in  $\Theta_i$  and  $\Theta_j$  but none in  $\Theta_k, k \neq i, k \neq j$  and so on.

$$(42) \quad I_{\Theta_i} = \sum_{j=0}^{n-1} \sum_{k_1, \dots, k_j \in \llbracket 1, n \rrbracket_j \setminus \{i\}} I_{\Theta_i \wedge \Theta_{k_1} \wedge \dots \wedge \Theta_{k_j} \setminus \Theta_{k_{j+1}}, \dots, \Theta_{k_n}}$$

where  $\llbracket 1, n \rrbracket_j$  is a draw of  $j$  indices without replacement in  $\llbracket 1, n \rrbracket$ . For  $j = 1 \dots n$ ,

$$(43) \quad I_{A_j} = \sum_{k_1, \dots, k_j \in \llbracket 1, n \rrbracket_j} I_{\Theta_{k_1} \wedge \Theta_{k_2} \wedge \dots \wedge \Theta_{k_j} \setminus \Theta_{k_{j+1}}, \dots, \Theta_{k_n}}$$

Then

$$(44) \quad \sum_{i=1}^n I_{\Theta_i} = \sum_{i=1}^n \sum_{j=0}^{n-1} \sum_{k_1, \dots, k_j \in \llbracket 1, n \rrbracket_j \setminus \{i\}} I_{\Theta_i \wedge \Theta_{k_1} \wedge \dots \wedge \Theta_{k_j} \setminus \Theta_{k_{j+1}}, \dots, \Theta_{k_n}}$$

In this sum, the term  $I_{\Theta_1 \wedge \Theta_2 \wedge \dots \wedge \Theta_n}$  appears  $n$  times, the terms  $I_{\Theta_1 \wedge \dots \wedge \Theta_{i-1} \wedge \Theta_{i+1} \wedge \dots \wedge \Theta_n}$  appear  $n - 1$  times, so we obtain the desired result.  $\square$

## APPENDIX C: EXISTENCE OF THE SOLUTION

The existence of the solution to  $(P_n)$  can be guaranteed in the following situation. Let us suppose that  $T$  is a metric space, and let us denote by  $B_a$  a ball (closed or open) of fixed radius  $L$  in  $T$  centered on  $a \in T$ .

LEMMA C.1. *Assume  $T$  is a finite dimensional Riemannian manifold (or more restrictively a finite product of  $\mathbb{S}^1$  (angles) and  $\mathbb{R}$  (actions).) Let us suppose that  $\mathcal{A} = \{B_{a_1}, \dots, B_{a_n}, k = 1, \dots, n_{max}, a_1, \dots, a_k \in T_0^k\}$  where  $T_0$  is a compact subset of  $T$ . Then the maximisation problem  $(P_n)$  has a (not necessarily unique) solution.*

PROOF. Note first that if the posterior probability is regular enough (non-singular with respect to Lebesgue measure), which we assume, the problem consists in maximizing, for each  $n$ , a linear combination of integrals of this distribution over sets in  $\mathcal{A}$ . As the center  $a_i$  move continuously, the integration sets  $A_i$  move continuously (in the Hausdorff topology for instance), and integration over them is continuous. Thus we are maximizing a continuous functional.

Let us first show that the problem has a solution for each fixed  $n$ . The set of candidates is a smooth manifold, and the dependence of the functional to maximize is through integrating a probability distribution over sets of fixed diameters. As the centers  $a_i$  of the balls go to infinity, the probability distribution has to become very small, and so does its integrals over fixed-sized balls; thus the value of the function to maximize goes to 0 as the parameters go to infinity. Since the functional is positive and non-zero, there is some  $\epsilon > 0$  such that the set on which the functional is bigger than  $\epsilon$  is compact. The functional, being continuous, attains its maximum on this set and this is then necessarily a global maximum. Then the maximum for  $0 \leq n \leq n_{max}$  is a maximum of  $(P_n)$ . (Or if  $n$  is not bounded, the values of the integrals of the posterior distribution as a function of  $n$  have to decrease to 0 uniformly since the whole probability distribution sums to 1, so by the same argument as above the maximum is attained for bounded  $n$ .)  $\square$

## APPENDIX D: PROOF OF LEMMA 2

LEMMA D.1. *Let us suppose that  $(P_n)$  has a solution  $\Theta_1^n \in T, \dots, \Theta_n^n \in T$ , with  $I_{\Theta_1^n} \geq \dots \geq I_{\Theta_n^n}$ . Then the solution to  $(P_{n+1})$  is either  $(\Theta_1^n, \dots, \Theta_n^n, \Theta_{n+1}^*)$  or such that  $\forall i \in \llbracket 1, n+1 \rrbracket, \exists j \in \llbracket 1, n \rrbracket$  such that  $\Theta_i^{n+1} \cap \Theta_j^n \neq \emptyset$ .*

PROOF. The proof relies on the simple property (P1): if a function  $f : E \rightarrow \mathbb{R}$  attains its maximum in a set  $X$ , then  $\forall D \subset E$  such that  $X \cap D = \emptyset$ , the set of solution to  $\arg \max_{x \in E \setminus D} f(x)$  is  $X$ .

Let us consider  $\Theta_{n+1} \in T$ . The solution to  $(P_{n+1})$  can be written as

$$(45) \quad \arg \max_{\substack{\Theta_1 \in T \setminus \Theta_{n+1}, \dots, \Theta_n \in T \setminus \Theta_{n+1} \\ \forall i, j \in \llbracket 1, n \rrbracket, i \neq j, \Theta_i \cap \Theta_j = \emptyset}} I_{\Theta_{n+1}} + \sum_{i=1}^n I_{\Theta_i}.$$

Either  $\forall i \in \llbracket 1, n \rrbracket, \Theta_{n+1} \cap \Theta_i^n = \emptyset$  then thanks to (P1), for  $E = T^n$  and  $D = \{x_1, \dots, x_n \in T^n, \forall i, x_i \notin \Theta_{n+1}^n\}$

$$(46) \quad \arg \max_{\substack{\Theta_1 \in T \setminus \Theta_{n+1}, \dots, \Theta_n \in T \setminus \Theta_{n+1} \\ \forall i, j \in \llbracket 1, n \rrbracket, i \neq j, \Theta_i \cap \Theta_j = \emptyset}} \sum_{i=1}^n I_{\Theta_i} = (\Theta_i^n)_{i=1..n}$$

As a consequence,

$$(47) \quad \arg \max_{\Theta_{n+1} \in T \setminus \bigcup_{i=1}^n \Theta_i^n} \arg \max_{\substack{\Theta_1 \in T \setminus \Theta_{n+1}, \dots, \Theta_n \in T \setminus \Theta_{n+1} \\ \forall i, j \in \llbracket 1, n \rrbracket, i \neq j, \Theta_i \cap \Theta_j = \emptyset}} I_{\Theta_{n+1}} + \sum_{i=1}^n I_{\Theta_i} = (\Theta_1^n, \dots, \Theta_n^n, \Theta_{n+1}^*)$$

up to a permutation of the indices (see remark B). If  $\exists i \in \llbracket 1, n+1 \rrbracket, \forall j \in \llbracket 1, n \rrbracket \in \Theta_i \cap \Theta_j^n = \emptyset$  then the same argument applies and the solution to  $(P_{n+1})$  is  $(\Theta_1^n, \dots, \Theta_n^n, \Theta_{n+1}^*)$ .

Let us denote by  $\neg P$  the negation of a proposition  $P$ . Since  $\neg(\exists i \in \llbracket 1, n+1 \rrbracket, \forall j \in \llbracket 1, n \rrbracket, \Theta_i \cap \Theta_j^n = \emptyset) = \forall i \in \llbracket 1, n+1 \rrbracket, \exists j \in \llbracket 1, n \rrbracket, \Theta_i \cap \Theta_j^n \neq \emptyset$ , and the union of the two cases account for all cases, we obtain the desired result.  $\square$

#### APPENDIX E: PROOFS OF THE RESULTS OF SECTION 4.2

We define  $u_n^y$  and  $v_n^y$  as in Eq. (14) and Eq. (15).

LEMMA E.1.  $\forall y$  in the sample space (i) the sequence  $(u_n^y)_{n=1..n_{max}}$  is increasing.

PROOF. (i) Let us suppose that there exists  $n$  such that  $u_{n+1}^y < u_n^y$ . That is

$$(48) \quad n+1 - \sum_{i=1}^{n+1} I_{\Theta_i^{n+1}} < n - \sum_{i=1}^n I_{\Theta_i^n}$$

This is equivalent to

$$(49) \quad 1 + \sum_{i=1}^n I_{\Theta_i^n} < \sum_{i=1}^{n+1} I_{\Theta_i^{n+1}}$$

Let us denote by  $i_0$  an index such that  $i_0 = \arg \max_{i=1..n+1} I_{\Theta_i^{n+1}}$ . Then

$$(50) \quad 1 \leq 1 + \sum_{i=1}^n I_{\Theta_i^n} - \sum_{i=1, i \neq i_0}^{n+1} I_{\Theta_i^{n+1}} < I_{\Theta_{i_0}^{n+1}}$$

Where the left inequality stems from the definition of the  $\Theta_i^n$  and  $\Theta_i^{n+1}$ . Indeed, by definition  $\sum_{i=1}^n I_{\Theta_i^n}$  is the maximum sum of probability mass on  $n$  disjoint  $\Theta_i$ ,

$$(51) \quad \sum_{i=1}^n I_{\Theta_i^n} \geq \sum_{i=1, i \neq i_0}^{n+1} I_{\Theta_i^{n+1}}.$$

We then have  $1 < I_{\Theta_{i_0}^{n+1}}$ , which is absurd.  $\square$

The statement and proof of Lemma E.2 are as follows. The fact that  $v_n^y$  (see Eq. (15)) is decreasing is evident from its definition.

LEMMA E.2. For a given posterior probability such that  $(u_{n+1} - u_n)_n$  is increasing, we can find an increasing function  $\gamma(x) > 0$  such that the solution of the maximum utility problem (7) solves the constrained problem (13).

PROOF. With the notation above, we have seen that  $u_n$  is increasing,  $u_n - u_{n-1}$  is increasing,  $v_n$  is decreasing, and  $v_{n-1} - v_n$  is decreasing. Those values depend only on the posterior probability function and on  $n$ . Let us fix  $x > 0$ . The constrained problem is

$$\min v_n \quad \text{subject to } u_n \leq x$$



while the maximum utility problem can be rewritten as

$$\min \left( v_n + \frac{1}{\gamma} u_n \right).$$

Since  $u_n$  is increasing, there is a highest  $n_0 = n(x)$  such that some configuration satisfies the constraint, i.e. such that  $u_{n_0} \leq x$ . Since  $v_n$  is decreasing, the solution of the constrained problem is found for  $n = n_0$ , for any configuration satisfying the constraint. We want to choose  $\gamma$  such that the solution of the maximum utility problem is also at  $n_0$ , for a configuration satisfying the constraint. We show that we can choose  $\gamma$  such that taking  $n \neq n_0$  leads to a larger value of  $v_n + \frac{1}{\gamma} u_n$ .

For  $n < n_0$ , we will have

$$v_n + \frac{1}{\gamma} u_n > v_{n_0} + \frac{1}{\gamma} u_{n_0}$$

if we take

$$(52) \quad \gamma > \frac{u_{n_0} - u_{n_0-1}}{v_{n_0-1} - v_{n_0}}.$$

For  $n > n_0$ , we will have

$$v_n + \frac{1}{\gamma} u_n > v_{n_0} + \frac{1}{\gamma} u_{n_0}$$

if

$$\gamma < \frac{u_{n_0+1} - u_{n_0}}{v_{n_0} - v_{n_0+1}}.$$

These two conditions can be satisfied since

$$\frac{u_{n_0} - u_{n_0-1}}{v_{n_0-1} - v_{n_0}} < \frac{u_{n_0+1} - u_{n_0}}{v_{n_0} - v_{n_0+1}}.$$

Choosing  $\gamma$  between those two bounds gives it as an increasing function of  $n_0$ , thus as an increasing function of  $x$ .  $\square$

The statement and proof of Lemma (E.3) are as follows.

LEMMA E.3. *If  $\forall n > 0, \exists i_0, \forall j = 1..n-1, \Theta_{i_0}^{n+1} \cap \Theta_j^{n-1} = \emptyset$ , the sequence  $(u_{n+1}^y - u_n^y)_{n=1..n_{max}}$  is increasing.*

PROOF. Let us suppose that  $\exists n \geq 1$  such that  $u_{n+1}^y - u_n^y < u_n^y - u_{n-1}^y$ . Replacing by the explicit expression of  $u_n$ , the inequality is equivalent to

$$(53) \quad \sum_{i=1}^n I_{\Theta_i^n} - \sum_{i=1}^{n+1} I_{\Theta_i^{n+1}} < \sum_{i=1}^{n-1} I_{\Theta_i^{n-1}} - \sum_{i=1}^n I_{\Theta_i^n}$$

By hypothesis,  $\exists i_0, \forall j = 1..n-1, \Theta_{i_0} \cap \Theta_j^{n-1} = \emptyset$ , Eq. (53) can be written

$$(54) \quad \sum_{i=1}^n I_{\Theta_i^n} - \sum_{i=1, i \neq i_0}^{n+1} I_{\Theta_i^{n+1}} < I_{\Theta_{i_0}^{n+1}} + \sum_{i=1}^{n-1} I_{\Theta_i^{n-1}} - \sum_{i=1}^n I_{\Theta_i^n}$$

The term  $I_{\Theta_{i_0}^{n+1}} + \sum_{i=1}^{n-1} I_{\Theta_i^{n-1}}$  is a sum of  $n$   $I_{\Theta_i}$  with disjoint  $\Theta_i$ . By definition of  $\Theta_i^n$ , the right hand side of the inequality is less than or equal to 0 and the left hand side of the inequality is greater than or equal to 0, which is absurd.

If  $\forall i = 1..n+1, \exists j = 1..n-1, \Theta_i^{n+1} \cap \Theta_j^{n-1} \neq \emptyset$ . In that case, we also have  $\forall i, \exists j \in \llbracket 1, n \rrbracket \Theta_i^n \cap \Theta_j^{n-1} \neq \emptyset$ , otherwise due to lemma 3.2 this would lead to a contradiction.  $\square$